Si Tran Nguyen Nguyen, Jinzhe Gong, Martin F. Lambert, Aaron C. Zecchin, Angus R. Simpson

Least squares deconvolution for leak detection with a pseudo random binary sequence excitation

Mechanical Systems and Signal Processing, 2018; 99:846-858

Final publication at http://dx.doi.org/10.1016/j.ymssp.2017.07.003

Least squares deconvolution for leak detection with a pseudo random binary sequence excitation

Si Tran Nguyen Nguyen, Jinzhe Gong, Martin F. Lambert, Aaron C. Zecchin, Angus R. Simpson

School of Civil, Environmental and Mining Engineering, University of Adelaide, SA 5005, Australia

Abstract

Leak detection and localisation is critical for water distribution system pipelines. This paper examines the use of the time-domain impulse response function (IRF) for leak detection and localisation in a pressurised water pipeline with a pseudo random binary sequence (PRBS) signal excitation. Compared to the conventional step wave generated using a single fast operation of a valve closure, a PRBS signal offers advantageous correlation properties, in that the signal has very low autocorrelation for lags different from zero and low cross correlation with other signals including noise and other interference. These properties result in a significant improvement in the IRF signal to noise ratio (SNR), leading to more accurate leak localisation. In this paper, the estimation of the system IRF is formulated as an optimisation problem in which the l_2 norm of the IRF is minimised to suppress the impact of noise and interference sources. Both numerical and experimental data are used to verify the proposed technique. The resultant estimated IRF provides not only accurate leak location estimation, but also good sensitivity to small leak sizes due to the improved SNR.

Keywords: Leak detection, linear system deconvolution, pseudo random binary sequence excitation, PRBS, water pipeline, hydraulic transient,

water distribution systems

1. Introduction

Underground water distribution pipeline systems represent critical infrastructure for modern cities. The maintenance of this infrastructure poses a major challenge as the pipelines are often buried underground. There has been growing attention to address this and many techniques for pipeline defect detection and condition assessment have been proposed [1, 2]. Typical defects of an aging pipeline include the leaks, blockages and internal and/or external corrosion in the pipes.

Leakage in water distribution systems can lead to significant economic cost due to water loss and associated additional energy consumption [3]. In addition, potential health risks to users due to pathogen intrusion during low pressure events [4]. Many leak detection techniques for water pipe systems have been developed and a selective literature review of leak detection techniques is presented in [5]. Hydraulic transient-based methods are relatively new techniques for leak detection and condition assessment of water pipeline systems. Since the original paper by Liggett et al. [6], researchers have continued to examine the interaction of transient pressure waves with leaks and blockages. The developed approaches can be sub-divided into time-domain-based, the frequency-domain-based techniques and time-frequency domain based techniques.

The time-domain techniques for leak detection mainly include time-domain reflectometry (TDR) techniques, impulse response function (IRF)-based methods, and inverse transient analysis (ITA) methods. Silva et al. [7] discussed TDR techniques for leak detection in which a pulse time delay was measured to compute the location of leak in the pipe. Later, Brunone and Ferrante [8], presented a method to detect a leak using a step transient pressure wave. The IRF-based methods were discussed in [9, 10], assuming the water pipe system was a linear time invariant (LTI) system. Thus, the measured output is the convolution of the input and the system impulse response. Given the measured input and output, one can estimate the IRF of a LTI pipe system, from which the leak locations can then be determined. With the ITA for leak detection [11, 12, 13, 14], the pressure responses at one or more locations are recorded during a transient event. A numerical pipeline model (with one or multiple leaks) is then iteratively calibrated to match the numerical pressure responses with the measured results. The success of ITA-based leak detection heavily relies on an accurate forward simulation, which is challenging for real pipes due to pipeline parameter uncertainties [13] and [15].

In the frequency-domain, the location and size of a leak can be inferred from the pipeline system frequency response diagram (FRD). The existence of a leak will introduce a sinusoidal pattern in the resonant or the anti-resonant peaks in an FRD, depending on the boundary condition of the pipeline system [16]. Early studies of FRD-based leak detection are reported in [17, 18]. Covas et al. [19] and Lee et al. [20] used the leak-induced sinusoidal pattern in the resonant peaks to gain an understanding of the system while Sattar et al. [21] proposed to use the leak-induced pattern in anti-resonant responses. Recently, Gong et al. [22] proposed a FRD-based leak detection technique that only uses the first three resonant peaks. However, accurate extraction of the FRD of a pipeline is challenging, especially when the pipe is embedded in a complex network. Zecchin et al. [23] used a frequency-domain approach for estimation of pipe network parameters using the maximum likelihood estimator. This was extended in [24] to the use of the expectation maximisation algorithm to deal with unmeasured boundary conditions.

Early research on leak detection based on Cepstrum has been shown to effectively locate a leak in a network [25, 26]. In addition, a wavelet transform was also used for leak detection research and reported in [27, 18, 28, 29, 29, 30]. In [31], empirical mode decomposition was used for leak detection using transient step excitation to the system, and the extracted feature was then mapped to the time-domain to localise the leak. These techniques can be classified as the time-frequency based approach.

When compared to the FRD-based techniques, in which the system is typically required to enter a steady oscillatory condition for the extraction of the response of the whole system [32], the time-domain IRF technique relies on the analysis of only the primary wave reflections from leaks for detection and localisation. The application of some FRD-based leak detection methods is restricted to simple pipe system configurations, such as a reservoir-pipeline-reservoir or reservoir-pipeline-valve system, because the FRD of a more complex system is difficult to interpret and derived relationships for the simple system will break down. The restriction on system complexity can be relaxed if the time-domain IRF method is to be used, since the particular segment of signal that contains the primary leak reflections can be extracted for independent analysis, while the wave reflections due to boundaries and network connections can be truncated. Hence, the time-domain IRF approach is preferable to be used for leak detection for specific pipe sections in a complex network.

The time-domain leak detection using IRF provides a straightforward interpretation of where the anomalies (e.g. leaks or blockages) are located. Despite the merits, IRF-based leak detection techniques have not been widely adopted in the field. In early works (e.g., [33]), a typical simple step wave was generated as the excitation signal using a fast valve closure operation. However, the step signal is not robust to system noise and other interference sources, which can lead to high false alarm rates [34].

The use of pseudo random binary sequence (PRBS) for IRF estimation and then leak detection was first discussed in [9]. However, only numerical experimentation was used for verification and the technique used for the estimation of the IRF was not robust against the noise and interference sources: the IRF was determined based on the division of the output signal by the input in the frequency domain followed by an inverse Fourier transform, referred to as the spectral division technique. This approach whilst simple to implement, can potentially amplify the small noisy components at certain frequencies in the denominator, especially for PRBS excitation signal, leading to an increase in the noise level in the IRF estimate and potential false detections. Further discussion of the PRBS spectral characteristic is discussed in section 2 illustrating the zero power frequencies of the PRBS at the clock frequency and its harmonics.

In the current research, a specific type of PRBS signal, the Inverse Repeat Pseudo Random Binary Sequence (IRS), is used as the excitation. This type of signal is very robust to system noise and other interference sources due to its correlation property. Furthermore, the IRS is antisymmetric in each period, which helps to reduce the effect of nonlinear system responses to the determination of linear system response functions [35]. The IRF estimate proposed in this paper is performed in the time domain by solving a least squares deconvolution problem. An optimisation problem is formulated seeking to minimise the least squares error and the l_2 norm of the IRF to allow suppression of the impact of noise and interference sources. The objective function is convex, leading to a unique solution that is independent of initialisations and a closed-form solution can be obtained. Numerical and experimental verifications are presented in this paper to illustrate the robustness and effectiveness of the proposed method against various sources of interference. A comparison of the new method is made with the conventional Cepstrum method [25] using both numerical and laboratory data.

2. Pseudo Random Binary Sequence excitation and problem formulation

The PRBS signal is commonly used in the electrical and electronics fields for identifying an electrical systems properties [36]. The signal offers greater robustness against the effect of noise in the system compared to step excitations as commonly used in both electrical [37, 38] and hydraulics [22] applications. Figure 1 illustrates the (a) time and (b) frequency responses of the IRS (a specific type of PRBS) [36] which will be used throughout in this paper. The IRS signal used throughout in this paper is designed to have one period of 20.46 s and a 3 dB bandwidth of 50 Hz. The pressure signal generation is described in [32] by the movement of two solenoids which control the valve opening and closing. The solenoid movement is measured by a linear voltage displacement transducer (LVDT) during the signal generation, which is used to approximate the input signal to the system. Figure 2 illustrates an example of anomaly identification in pipelines based on transient analysis in the time domain. A reservoir-pipeline-valve system configuration is considered in Fig. 2 as it facilitates the numerical simulations to be discussed. An excitation pressure signal similar to that in

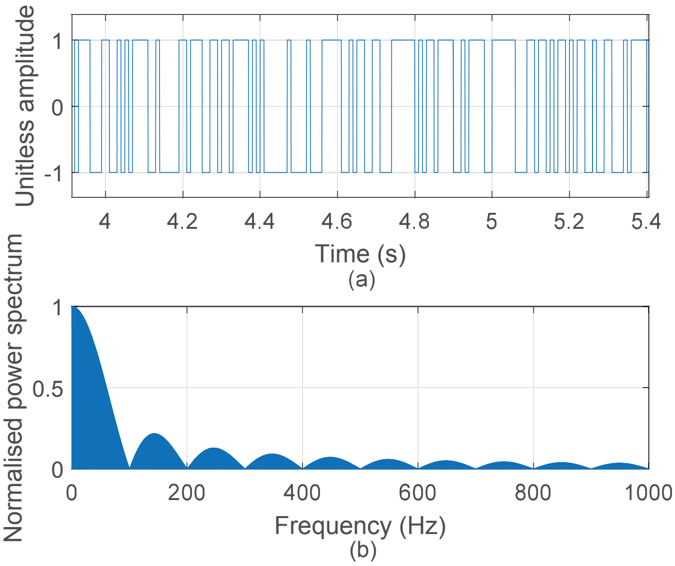

Figure 1: The time domain of the IRS (a) and corresponding frequency spectrum (b). One period of the IRS corresponds to 20.46 s.

Fig. 1(a), denoted as $s(t)$, is generated as an input to the water pipeline system (Fig. 2), which is an approximation of the IRS valve movement pattern. For simplicity, it is assumed that signal dissipation and dispersion are negligible when the transient signal $s(t)$ travels in the pipeline towards the anomalies at distances $d_1, d_2, \cdots, d_N$ from the point of signal generation and measurement. As discussed, the anomalies within the pipe will cause reflections of the excitation wave $s(t)$, which will be measured by a pressure sensor positioned at the point of signal generation. The received signal at the sensor, denoted as $r(t)$, is the superposition of the excitation signal and the reflected signals caused by anomalies, which can be written as

$$r(t) = s(t) + \sum_{i=1,\cdots,N} R_i s(t - \tau_i), \tag{1}$$

for R_i representing the reflection coefficient, indicating the ratio between energy of the reflected wave at the anomalies and the incident wave's, τ_i being the time taken for the transient pressure to travel to the anomalies and back to be measured by the sensor; $\tau_i = 2d_i/a$ where a is the transient pressure wave speed. Note that higher order reflections are neglected (i.e. reflections resulting from an already reflected wave), as they are typically significantly smaller in magnitude, with reflection coefficients on the order of R^3, R^5, etc., where $R < 0.2$ are typical for pipeline anomaly detection applications. The problem of detection and localisation of the anomalies in the pipe is equivalent to estimating the reflection coefficient R_i and the time delay τ_i of the equation (1), whose concept is similar to the conventional time-domain reflectometry based method [39].

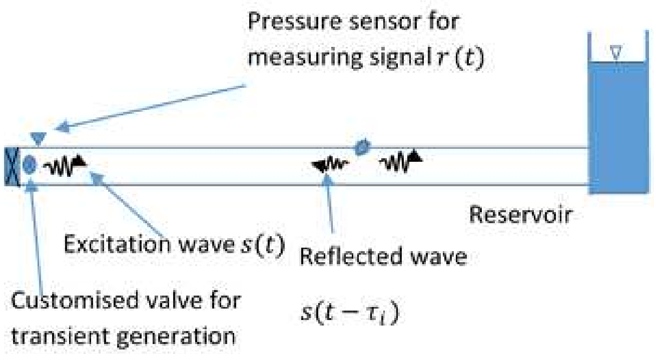

Figure 2: Transient-based strategy for anomaly identification in a pipeline.

3. Least squares deconvolution for water pipeline system identification

A pipeline system can be considered as an approximate Linear Time Invariant (LTI) system for an appropriate magnitude level of transient excitation [22]. Therefore, if the input to the system is denoted as $x(t)$ and the output as $y(t)$, the relationship between the input and output signals is given by

$$y(t) = \int_{-\infty}^{+\infty} h(\tau)x(t-\tau)d\tau \quad (2)$$

where $h(t)$ is the impulse response function (IRF) of the system - describing the dynamic properties of the system in consideration. Eq. (2) represents the convolution operation of the two signals $h(t)$ and $x(t)$ in the time domain. In the frequency domain, this relationship can be expressed as $Y(f) = H(f)X(f)$, for signals $X(f), H(f)$, and $Y(f)$ representing the Fourier transforms of the time domain signal $x(t), h(t)$, and $y(t)$, respectively.

To compute a system transfer function in the frequency domain given the input and output signals, conventionally a simple division operation is applied, given by

$$H(f) = Y(f)/X(f) \quad (3)$$

for $H(f)$ being the system transfer function, which is the Fourier transform of the IRF $h(t)$. An issue can be found using this spectral division approach if the input signal spectrum contains zero frequency components such as the IRS signal in Fig. 1(b). Thus, division by this signal in frequency domain will cause the inversion of zero value at certain frequencies. This is caused by the line spectrum characteristic of IRS, whose spectrum only has energy at some specific frequencies [examples of these zero energy frequencies can be observed at 100, 200 Hz, etc. (the clock frequency and its harmonics), in Fig. 1(b)].

To address this issue, a time-domain technique is proposed. Consider the discretised version of the signals in the convolution operation in Eq. (2), in the discrete time domain it can be expressed as

$$y[n] = \sum_{k=1}^{N} h[k]x[n-k+1]. \tag{4}$$

The expression in Eq. (4) is a linear operation which can be represented by a matrix multiplication, formulated as

$$\mathbf{y} = \mathbf{X}\mathbf{h}. \tag{5}$$

The signal $\mathbf{y}$ is a $N \times 1$ column vector representing the output signal $y[n]$, $\mathbf{X}$ being the $N \times N$ convolution matrix constructed using the input signal $x[n]$ and $\mathbf{h}$ being the $N \times 1$ column vector representing the impulse response function in discrete time domain. The convolution matrix $\mathbf{X}$ and column vector $\mathbf{y}, \mathbf{h}$ are constructed as follow:

$$\begin{aligned}
\mathbf{X} &= \begin{bmatrix} \mathbf{x}[1] & 0 & 0 & \cdots & 0 \\ \mathbf{x}[2] & \mathbf{x}[1] & 0 & \cdots & 0 \\ \mathbf{x}[3] & \mathbf{x}[2] & \mathbf{x}[1] & \cdots & 0 \\ \vdots & \vdots & \vdots & \ddots & \vdots \\ \mathbf{x}[N] & \mathbf{x}[N-1] & \mathbf{x}[N-2] & \cdots & \mathbf{x}[1] \end{bmatrix} \\
\mathbf{y} &= \begin{bmatrix} \mathbf{y}[1] & \mathbf{y}[2] & \mathbf{y}[3] & \cdots & \mathbf{y}[N] \end{bmatrix}^T \\
\mathbf{h} &= \begin{bmatrix} \mathbf{h}[1] & \mathbf{h}[2] & \mathbf{h}[3] & \cdots & \mathbf{h}[N] \end{bmatrix}^T
\end{aligned} \tag{6}$$

where superscript T represents the transpose operation. The impulse response $\mathbf{h}$ will be computed by solving a linear equation system Eq. (5), given by

$$\mathbf{h} = \mathbf{X}^{-1}\mathbf{y}, \tag{7}$$

for an invertible matrix $\mathbf{X}$, which is not the case in all scenarios.

To reduce the effect of noise sources in the pipeline system, a least squares optimisation for the IRF estimation is proposed to estimate the IRF $\mathbf{h}$ given the input matrix $\mathbf{X}$ and output vector $\mathbf{y}$, whose objective function is formulated as

$$f(\mathbf{h}) = \|\mathbf{y} - \mathbf{X}\mathbf{h}\|_2^2 + \lambda\|\mathbf{h}\|_2^2 \tag{8}$$

where $\mathbf{h}, \mathbf{X}, \mathbf{y}$ represent the impulse response function, input matrix and output of the system, defined as in Eq. (6); λ determines the weighting ratio between the two terms in Eq. (8). Minimising $f(\mathbf{h})$ in Eq. (8) effectively minimises the energy of the impulse response, $\|\mathbf{h}\|_2^2$, and simultaneously minimising the least squares error term, defined by $\|\mathbf{y} - \mathbf{X}\mathbf{h}\|_2^2$. Increasing the value λ effectively increases the weighting on regularisation $\|\mathbf{h}\|_2^2$, which suppresses the interference energy at the resultant IRF. This comes at the expense of a higher least squares error defined by $\|\mathbf{y} - \mathbf{X}\mathbf{h}\|_2^2$. If $\lambda = 0$, the problem becomes a conventional deconvolution problem as similar to that in Eq. (7). The second term of Eq. (8) $\|\mathbf{h}\|_2^2$ should only have energy at the time points where the anomalies reflections occur which is usually small since the reflected energy is small compared to the incident wave. Rewriting the function in Eq. (8) gives us:

$$f(\mathbf{h}) = (\mathbf{y} - \mathbf{X}\mathbf{h})^T(\mathbf{y} - \mathbf{X}\mathbf{h}) + \lambda\mathbf{h}^T\mathbf{h} \tag{9}$$

The first derivative $df/d\mathbf{h}$ is given as

$$df/d\mathbf{h} = -2\mathbf{y}^T\mathbf{X} + 2\mathbf{h}^T\mathbf{X}^T\mathbf{X} + 2\lambda\mathbf{h}^T \tag{10}$$

Equating $df/d\mathbf{h} = 0$ yields

$$\mathbf{h} = (\mathbf{X}^T\mathbf{X} + \lambda\mathbf{I})^{-1}\mathbf{X}^T\mathbf{y} \tag{11}$$

The matrix $\mathbf{I}$ represents the identity matrix. The expression in (11) gives the closed form solution for the optimum of objective function defined in (8), given the matrix $\mathbf{X}$, output $\mathbf{y}$ and λ. It should be noted that this approach can be used for non-invertible input matrix $\mathbf{X}$, in which case the solution of the IRF cannot be obtained using Eq. (7). For example, quite often the time interval of interest of the IRF (in the order of seconds, equivalent to the time taken to for the wave to travel to the boundary and back and sensor) is much smaller than the IRS period (20.46 s), thus the size of the vector $\mathbf{h}$ is much smaller than that of $\mathbf{y}$. This will result in the convolution matrix $\mathbf{X}$ being a non-square matrix and its inverse $\mathbf{X}^{-1}$ does not exist.

4. Experimental set-up and numerical verification

The following experimental configuration is used to test the performance of the proposed approach.

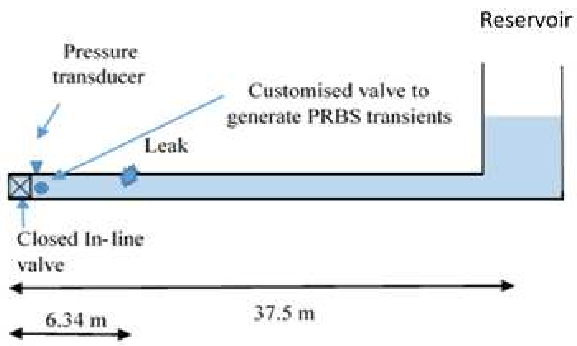

Figure 3: The experimental configuration of a valve-leak-reservoir system. The transient generator is located near the valve next to the pressure transducer, the leak is at 6.34 metres from the valve and the reservoir is at 37.5 metres.

The pipe system in Fig. 3 is located at the Robin Hydraulics Laboratory at the University of Adelaide. It is bounded by a closed in-line valve at one end and the reservoir at the other end with the pressure head of 38.5 metres. The pipe is made of copper with an internal diameter of 22.14 mm. A customised valve is connected to the pipe for IRS transient signals to be generated, located 145 mm from the closed in-line valve. The head response of the system is measured by a pressure transducer (Druck PDCR 810, Leicester, UK) mounted on the main pipe with a sampling rate of 5000 samples per second. A small orifice is used to simulate a leak in the pipe. As discussed in [32], the IRS signal is generated by the movement of two solenoids controlling the valves opening and closing and the solenoid movement. The movement is measured by a linear voltage displacement transducer (LVDT) to estimate the input signal to the system.

The configuration used in Fig. 3 is considered to avoid the issue of directional wave propagation, referred to as the ambiguity issue of the reflected waves from the anomalies arriving at the sensor from multiple paths/directions. For such issue, pure time delay information cannot resolve the ambiguity. Whilst there exists techniques to resolve such issue [40], it is beyond the scope of this paper.

The following steps are taken for leak detection using the IRS excitation signal and least squares approach:

- Initialise the start time t_0. The IRS period in second given by $T_P = 20.46$ s and the sampling frequency is given by $F_s = 5000$ Hz. The corresponding samples per period is given by $[T_P F_s]$; $[.]$ represents the integer rounding operation.

- Let $T[n], R[n]$ be the discrete time signals representing the solenoids manoeuver and the measured head pressure at the transducer, respectively, the input $x[n]$ and output $y[n]$ to the LTI system in consideration is given by:

$$\begin{cases} x[n] = T[n+n_0] \\ y[n] = R[n+n_0], \end{cases}$$

for $n = 1, \cdots, N_p; n_0 = [t_0 F_s]$.

- The discrete signals $x[n]$, $y[n]$ will be used to construct the matrix $\mathbf{X}$ and column vector $\mathbf{y}$ as in (6), which will be then fed into the optimisation problem defined in (8), the optimum is given by (11).

4.1. Numerical verification

Using the method of characteristics (MOC) [41], numerical data is generated for the configuration in Fig. 3. The MOC, discussed in [41] offers a step-by-step method to solve the partial differential equations describing the relationship between the pressure head H and flow Q at a given time t and location x. The governing equations are given as:

$$\frac{\partial Q}{\partial x} + \frac{gA}{a^2}\frac{\partial H}{\partial t} = 0 \tag{12}$$

$$\frac{\partial H}{\partial x} + \frac{1}{gA}\frac{\partial Q}{\partial t} + \frac{fQ|Q|}{2gDA^2} = 0, \tag{13}$$

where a is the wave speed, A is the pipe cross-sectional area at the location x in consideration; D is the pipe diameter, f is the Darcy-Weisbach friction factor. The MOC solves the differential equations (12), (13) in discrete the time domain which gives a good approximation of the solutions, given a sufficiently small time step along the characteristic lines [41].

The pressure head at the transducer of the configuration in Fig. 3 is generated numerically as the customised valve's movement is controlled to follow an IRS pattern. The associated change in flow/pressure following the equations (12), (13) at the valve will result in an excitation wave (input to the system), which will approximate an IRS signal. The copper pipeline has internal diameter of 22.14 mm, an estimated wave speed of 1321 m/s and a simulated leak with diameter of 2 mm.

The input to the system is the approximation of the IRS signal as shown in Fig. 1. It should be noted the current version of the IRS generator used in the laboratory as described in [32] continuously generates a new period of IRS signal after it finishes the previous period. For consistency, the numerical data is designed to reflect this behaviour to be compared with the real data result in the next section.

One of the key challenges for this system is the long PRBS period of 20.46 s with respect to the short pipeline in consideration for the given nominal wave speed of 1321 m/s (with a pipeline return time of 56 ms). Therefore, the output signal of one period long of data measured by the transducer will consist of the superposition of multiple components including the incident wave actively generated by the PRBS generator, and multiple reflections from the leak, reservoir, closed in-line valve, secondary reflections from leak and reservoir, etc. These multiple reflected waves will interfere with each other since they are not well separated in time. Setting the start time t_0 to be 5 s, Fig. 4 illustrates the normalised IRF estimate for the numerical experiment using the least squares approach. It should be noted that the illustrated IRF in Fig. 4 is normalised by the magnitude of the first sample, which indicates the incident wave.

In Fig. 4(a), the estimated IRF illustrates the reflections from the leak at 0.0098 s, and from the water reservoir at 0.057 s. Therefore, the leak location found will be $(0.0098/0.057) \times 37.5 = 6.44$ metres from the in-line valve which is approximately the location of the known leak location of 6.34

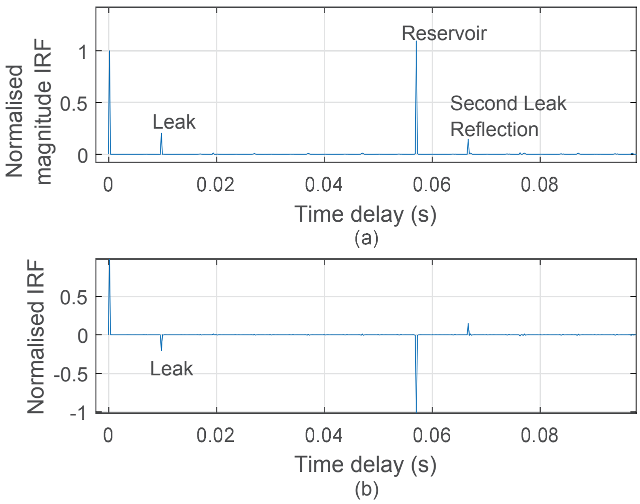

Figure 4: The normalised magnitude of the estimated IRF (a) and the normalised IRF including the signs at the reflections (b) from numerical data. The time delays of the reflections are found to be 0.0098 s (corresponding to the leak) and 0.057 s (corresponding to the pressurised reservoir).

metres (see Fig. 3). The error is due to the low sampling frequency of 5000 Hz, chosen to be consistent with experimental data to be presented in the laboratory verification section.

In Fig. 4, the normalised magnitude plot is presented in Fig. 4(a) to show the timings (location) that have energy, caused by the incidental and reflected waves. The IRF result is from a numerical experiment without interference, hence the IRF normalised magnitude plot shows no interference from the noise component, i.e., the energy at the other times different to the expected transient events is negligible. The bottom panel shows the actual sign of the IRF; the negative sign reflection in Fig. 4(b) indicates a reduction in transient pressure at the considered location, suggesting a leak instead of a blockage which would have an increase in transient pressure and hence positive IRF reflection. The second leak reflection can be observed as the transient wave reflects from the leak for the second time, the time difference between these two leak reflections is approximately the time for the wave to travel to the pressurised reservoir and back to the pressure transducer.

4.2. Comparison with the Cepstrum method

The MOC is again used to generate pressure head data at the sensor in the configuration 3 with the excitation signal similar to the Cepstrum method discussed in [25]. The normalised head is illustrated in Fig. 5 in blue solid trace whilst the solenoid valve movement is shown by the dashed trace.

If the normalised pressure in Fig. 5 is denoted as $\mathbf{x}$, the Cepstrum of $\mathbf{x}$ is given by $DFT\{\log\{DFT\{\mathbf{x}\}\}\}$; where $DFT\{.\}$ represents the discrete Fourier transform operation, $\log\{.\}$ represents the computation of natural logarithm operation. The Cepstrum of the normalised head pressure in Fig. 5(a) is illustrated in Fig. 5(c).

Figure 5(c) illustrates the Cepstrum of the normalised signal in Fig. 5. It should be noted that whilst a very good SNR can be achieved at the leak (at time 0.0096 s), there exists a strong artefact at 0.0472 s. It can be found that this artefact is related to the leak time as $0.0472 = 0.0568 - .0096$, where $0.0096, 0.0568$ s are the leak time delay and the reservoir delay, respectively. Consider the zoomed in plot of the normalised pressure signal $\mathbf{x}$ in Fig. 5(b). It should be noted Cepstrum of the time domain signal $\mathbf{x}$ searches for the regularity in the signal, i.e., the regular change in pressure in the time domain trace. In Fig. 5(b), it can be observed that at least three significant components in Cepstrum domain are expected (or time intervals in the original time domain) including: 1) the leak time delay (the

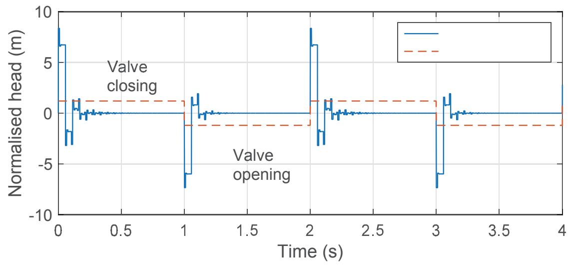

(a) Time-domain trace

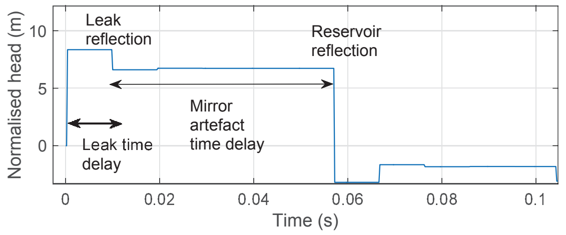

(b) Zoomed-in signal

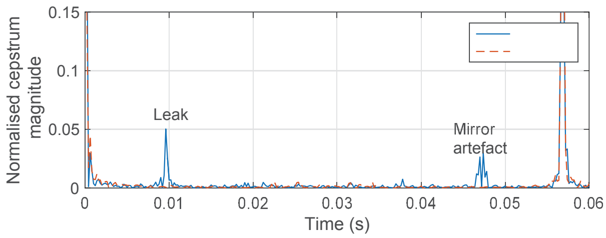

(c) Cepstrum

Figure 5: (a) Normalised head numerically generated using the MOC technique of the configuration in Fig. 3 (blue solid trace) and the corresponding movement of the solenoid valve (red dashed trace); (b) the zoomed-in signal of that in (a) and (c) Cepstrum; the blue solid trace represents the Cepstrum with a leak whilst red dashed trace represents one without a leak.

time interval between the rise/drop in pressure due to the solenoid valve closing/opening and the drop/rise in pressure due to the leak), 2) the time interval between the leak reflection and the reservoir reflection and 3) the time interval between the solenoid valve closing/opening and the change in pressure due to the reservoir. It should be noted that a numerical experiment has been made to move the leak location to different position along the pipeline and found that the artefact location has also moved accordingly.

The mirror artefact observed in Fig. 5(c) corresponds to the time interval between the change in pressure due to the leak and the change in pressure due to the water reservoir, which is dependent on the location of the leak (unknown) and the location of the reservoir (known). This artefact is embedded in the time domain signal, however, not corresponding to a wave reflection due to any anomaly. Further verification regarding this artefact is made using the laboratory test in the next section (a similar artefact at approximately the same time can be observed). The proposed least squares deconvolution seeks the location of the reflected wave, thus suppressing the effect of this mirror artefact.

5. Laboratory verification

Laboratory data is used to test the proposed algorithm. The experiments were conducted in the Robin Hydraulics Laboratory, University of Adelaide, Australia for the configuration illustrated in Fig. 3. All the experiments conducted lasted for 10 minutes, with the first few seconds of data measured under the steady state condition (with the side discharge valve open). The transient event is then started by triggering the IRS excitation.

5.1. Verification of the proposed method using laboratory data

Laboratory tests for IRS excitation signal with a discharge orifice size of 2 mm, 1 mm and an irregular orifice to simulate the leak (irregular leaks were simulated using a partially-opened side discharge valve). Discussion of the effect of irregular orifice to the system can also be found in [8, 42]. Multiple tests on different days were also considered for the verification. The IRS reference signal, measured by the LVDT (measuring the dynamic valve opening), and the pressure head, measured by the transducer mounted on the main pipe are illustrated in Fig. 6. In this experiment the reference signal measured by the LVDT is used as an approximation of the system input signal and was used to construct the input matrix $\mathbf{X}$ described in Eq. (6). Similarly, the output pressure measured by the transducer is heavily dependent on the device sensitivity to the frequency band of interest, its dynamic range and other practical instrumentation issues [43]. The pressure measurement at the transducer is used to construct the output column vector $\mathbf{y}$. The IRF result, as determined by the proposed least squares approach, is shown in Fig. 7.

In Fig. 7, the leak location can be clearly observed at approximately 0.0094 s together with those representing the incident wave at the beginning, the reflected wave caused by the reservoir at 0.0566 s and the second leak reflection at 0.066 s. The experimental IRF response is very similar to that of the numerical result suggesting the robustness against the aforementioned practical issues in application to a real pipe system using this method. The leak location can be computed as $0.0094/T \times L = 6.23$ metres compared to the actual location of 6.34 metres, for L being the pipe length which is equal to 37.5 m, T being the time taken for the transient wave to travel two pipe lengths from the signal generator to the reservoir and back to the transducer, given as 0.0566 s [refer to Fig. 7(a) reflection time of pressurised reservoir]. The sampling frequency for data acquisition for this experiment is 5000 Hz. Thus for the wave speed computed as $2L/T = 1325$ m/s, each sample

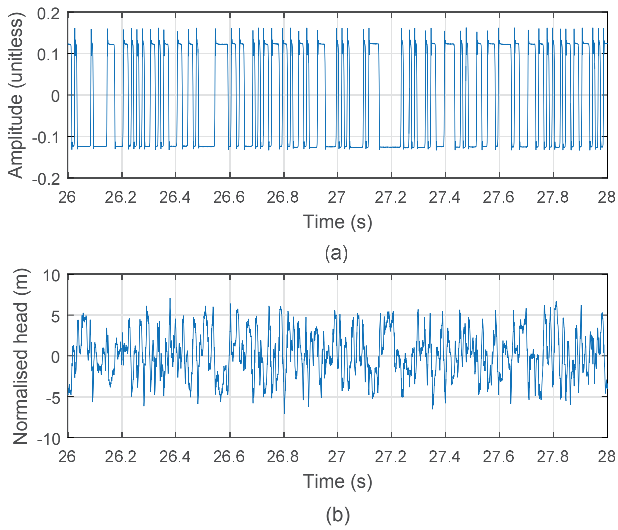

Figure 6: (a) The dimensionless IRS valve perturbation and (b) the pressure head measured by the pressure transducer (in a normalised form).

corresponds to a distance of $1325/5000 = 0.26$ metres. This effectively means that the leak location error computed by the proposed method is due to the low sampling frequency and not the algorithm error, since the next time sample of the IRF from the computed leak time corresponds to $6.23 + 0.26 = 6.49$ metres which is greater than the actual leak location of 6.34 metres.

The leak locations computed based on least squares IRF estimation for different datasets are given in Table 1 for T_0, T representing the timings of the leak and reservoir reflections, respectively. The estimation error is computed as $|L_{est} - L_{actual}|/L$ for L_{est}, L_{actual} being the estimated and actual distance from the in-line valve (transducer) to the leak, respectively. As seen by the low error in Table 1, the proposed least squares IRF estimation for IRS excitation has been shown effectively and accurately localise the

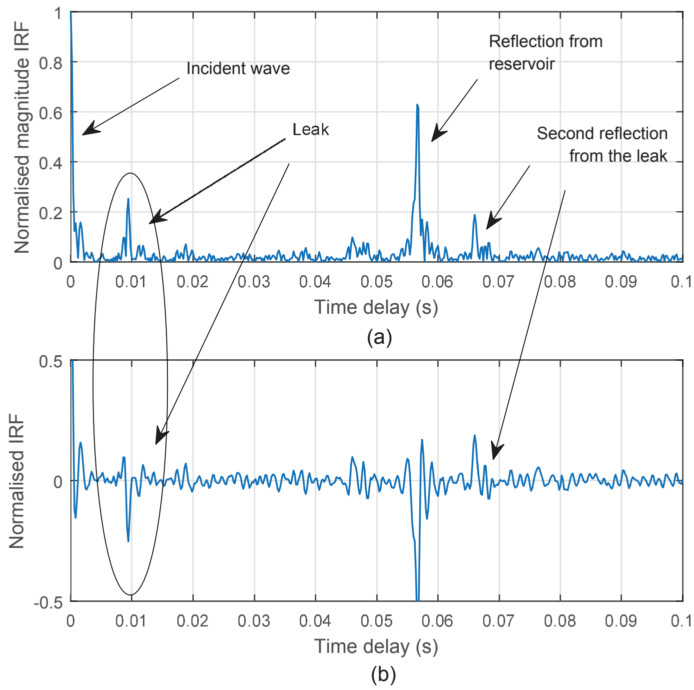

Figure 7: IRF estimate for laboratory data for 2 mm leak diameter: (a) normalised magnitude and (b) normalised amplitude.

location of leak in a pipeline system. Verifications were made using different tests with the simulated leak orifice varying from a circular orifice of 2 mm diameter (Test 1 repeat 1 and repeat 2 and Test 2), 1 mm diameter (Tests 3, 4) and an irregular orifice (Tests 5, 6). As seen in Table 1, the highest estimation error is 0.37%. Compared to the existing literature research using PRBS excitation for leak localisation in frequency domain [32] where an estimation error was reported to be of approximately 2% for a similar scale pipeline system, the proposed IRF estimation has significantly improved the accuracy. It should be noted that the higher error is obtained with the smaller leak diameter (1 mm) in which the reflection from leak is smaller

Data-set	$T_0; T$ (s)	Leak location (m)	Error (%)	Leak size diameter (mm)
Test 1-Repeat 1	0.0094;0.0568	6.206	0.35 %	2 mm
Test 1-Repeat 2	0.0094;0.0566	6.23	0.29 %	2 mm
Test 2-Repeat 1	0.0094;0.0566	6.23	0.29 %	2 mm
Test 3	0.0092;0.0566	6.1	0.37 %	1 mm
Test 4	0.0092;0.0566	6.1	0.37%	1 mm
Test 5	0.0094;0.0566	6.23	0.29 %	Irregular Orifice
Test 6	0.0094;0.0566	6.23	0.29 %	Irregular Orifice

Table 1: The tabulated results for leak localisation for various laboratory tests.

compared to the 2 mm diameter experiments.

5.2. Comparison with Cepstrum method using laboratory data

A comparison between the proposed approach and the Cepstrum method discussed in [25] is performed using laboratory data for the configuration in Fig. 3. The normalised pressure head is shown in Fig. 8 (a) with the rise in pressure at time 0 due to a valve closure. The drop in pressure at approximately 0.01 s is due to the leak. It should be noted that this pattern is similar to that observed in with the numerical counterpart in Fig. 5(b). One can argue that in an ideal environment such as that in Fig. 5(b), the leak can easily be observed and its time/location can be calculated from the time domain trace. In Fig. 8 (a), it can be observed that in a real scenario, the non-ideal movement of the solenoid valve used to generate the transient pressure and the system noise interference can lead to false-detection or mis-idenfication of the anomalies if purely using the time-domain trace. For example, in Fig. 8 (a), there are locations where the pressure perturbation does not correspond to any features in the pipe (at approximately 0.05 s).

The Cepstrum of the signal in Fig. 8 (a) is shown in Fig. 8 (b) whilst the least squares approach result is shown in Fig. 8 (c). An improved SNR can be observed by both approaches. A similar artefact can be observed in Fig. 8 (b) compared to that in Fig. 5(c) obtained from the numerical data. In Fig. 8 (c), the artefact is suppressed using the proposed algorithm with IRS excitation.

6. Application to a network configuration

For completeness, the following pipe network is considered for comparison between the proposed approach and the Cepstrum method [25], the configuration is shown in Fig. 9. Three pipe sections of copper material and internal diameter of 12.6 mm, the lengths are 8.5, 9 and 11 metres for pipe sections 1, 2 and 3, respectively. The pressurised tanks each have a pressure of 19 metres. A 1 mm diameter leak is located at approximately 9.5 metres from the pressure transducer on the pipe 3 section. An in-line valve was located at the boundary of pipe 1, next to a customised valve used to generate the transient pressure as seen in Fig. 9. The configuration and parameters are designed similar to that described in [25], except the use of the in-line valve instead of the inlet at the boundary of pipe 1. It is because the use of the reflection from the inlet would result in a destructive interference at the pressure transducer for the PRBS excitation.

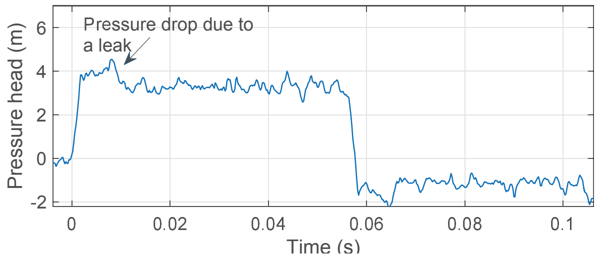

(a) Normalised head pressure

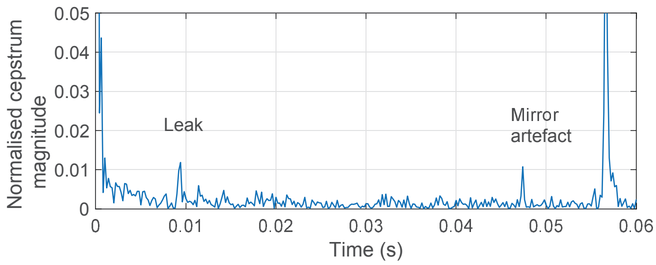

(b) Cepstrum of the signal in (a)

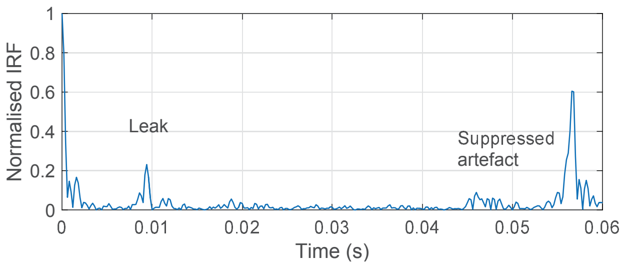

(c) Least squares deconvolution using IRS

Figure 8: Normalised head pressure (a); Cepstrum of the laboratory data (b) and impulse response function using the proposed least squares approach (c) of system of a 22.14 mm internal diameter copper pipeline and a 2 mm diameter leak.

The method of characteristics (MOC) is again used to generate the transient pressure at the pressure transducer for the configuration in Fig. 9 with the wave speed specified as 1447 m/s. The excitation to the system was

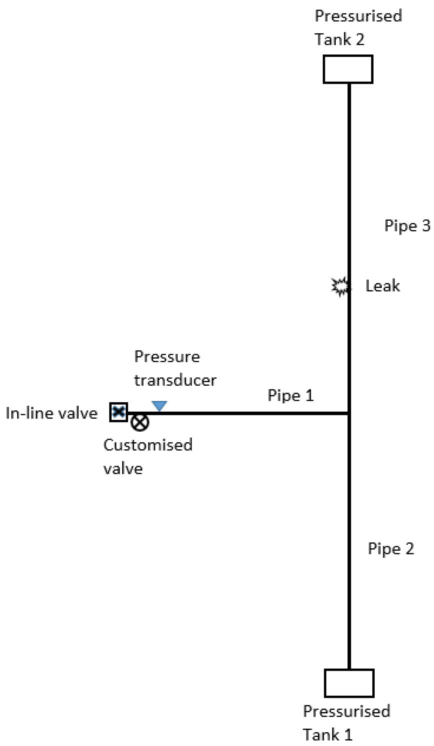

Figure 9: T network configuration.

generated similar to that described in [25] by a solenoid valve closing and opening periodically with the time period of 1 s. Data was generated for the structure with and without the leak. Both Cepstrum and least squares results are shown in Fig. 10 where the dashed traces represent the results without leak, solid traces are ones with leak.

From Fig. 10 (a) it could be seen that apart from the known features such as reflections from the junction, leak and pressurised tank 1 and 2, there exist other small artefacts in the Cepstrum results. Since this is a result of a numerically generated signal in which an ideal pressure rise/drop occurs at each time a change in impedance/flow occurs, the system can

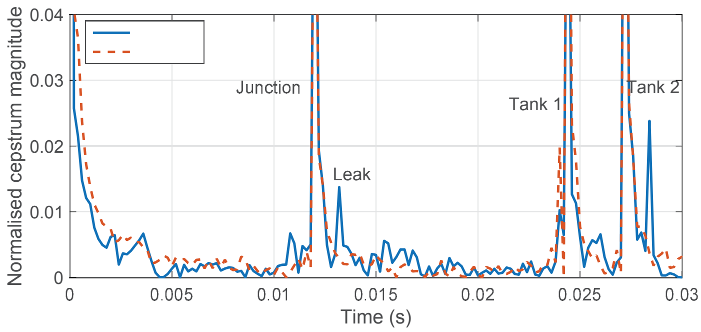

(a) Cepstrum method [25]

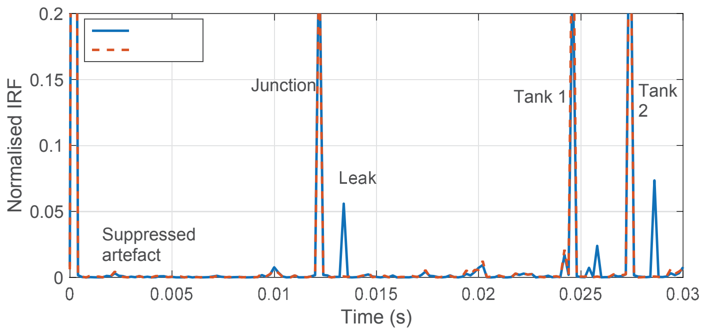

(b) Proposed least squares deconvolution (IRS)

Figure 10: The Cepstrum of the laboratory data (a) and impulse response function using the proposed least squares approach (b); in both figures the red dashed traces represent the results without leak whilst blue solid traces are those with a leak.

be considered to be free from noise interference. Therefore, the artefacts observed in the Cepstrum method are due to the interactions between the pressure changes in the time domain trace and its regularity, similar to that found for the single pipeline scenario, which becomes more complicated when there are more features in the configuration. It should be noted that the de-noising step described in [25] was omitted in the Cepstrum analysis since there exists no noise in the numerical data. In Fig. 10 (b), the artefacts are suppressed using the proposed approach. It is because the proposed least squares deconvolution with IRS excitation seeks for the reflected excitation wave which is different to the Cepstrum approach that searches for the regularity of change in the pressure trace.

7. Conclusion

This paper investigates the use of a new least squares deconvolution approach for impulse response function estimation for leak localization in a pipeline system. The PRBS excitation has been shown to significantly improve the signal to noise ratio for the IRF estimation, hence significantly improving the localization accuracy even for small leak sizes compared to the existing frequency domain counterpart [32]. The proposed method provides an elegant new way for detecting and localizing the leak in a water pipeline or simple network, which can be easily extended for other types of anomalies such as blockages and changes in pipe wall thickness a critical step leading to condition assessment of water pipes. Verification of the algorithms was made using both numerical and experimental data with various experimental datasets used to test the algorithm performance. The performance comparison has also been undertaken between the proposed approach and Cepstrum approach. A satisfactory suppression of the artefacts in the IRF could be obtained by using the proposed approach compared to Cepstrum. This was achieved by formulating the pipeline system deconvolution problem as a least squares optimisation problem with an l_2 regularisation.

Acknowledgement

The research presented in this paper has been supported by the Australian Research Council through the Discovery Project Grant DP140100994.

References

[1] M. Eybpoosh, M. Berges, H. Y. Noh, An energy-based sparse representation of ultrasonic guided-waves for online damage detection of pipelines under varying environmental and operational conditions, Mechanical Systems and Signal Processing.

[2] B. Vogelaar, M. Golombok, Quantification and localization of internal pipe damage, Mechanical Systems and Signal Processing 78 (2016) 107–117.

[3] A. F. Colombo, B. W. Karney, Energy and costs of leaky pipes: toward comprehensive picture, Journal of Water Resources Planning and Management 128 (6) (2002) 441–450.

[4] M. R. Karim, M. Abbaszadegan, M. LeChevallier, Potential for pathogen intrusion during pressure transients, Journal/American Water Works Association 95 (5) (2003) 134–146.

[5] R. Puust, Z. Kapelan, D. Savic, T. Koppel, A review of methods for leakage management in pipe networks, Urban Water Journal 7 (1) (2010) 25–45.

[6] J. A. Liggett, L.-C. Chen, Inverse transient analysis in pipe networks, Journal of Hydraulic Engineering 120 (8) (1994) 934–955.

[7] R. A. Silva, C. M. Buiatti, S. L. Cruz, J. A. Pereira, Pressure wave behaviour and leak detection in pipelines, Computers & chemical engineering 20 (1996) S491–S496.

[8] B. Brunone, M. Ferrante, Detecting leaks in pressurised pipes by means of transients, Journal of hydraulic research 39 (5) (2001) 539–547.

[9] P. J. Lee, J. P. Vtkovsk, M. F. Lambert, A. R. Simpson, J. Liggett, Leak location in pipelines using the impulse response function, Journal of Hydraulic Research 45 (5) (2007) 643–652. doi:10.1080/00221686.2007.9521800.

[10] J. Vitkovsky, P. J. Lee, M. L. Stephens, M. F. Lambert, A. R. Simpson, J. A. Liggett, Leak and blockage detection in pipelines via an impulse response method, Pumps, electromechanical devices and systems applied to urban water management 1 (2003) 423–430.

[11] D. Covas, H. Ramos, Case studies of leak detection and location in water pipe systems by inverse transient analysis, Journal of Water Resources Planning and Management 136 (2) (2010) 248–257.

[12] B. Jung, B. Karney, Systematic exploration of pipeline network calibration using transients, Journal of Hydraulic Research 46 (sup1) (2008) 129–137.

[13] J. P. Vitkovsy, M. F. Lambert, A. R. Simpson, J. A. Liggett, Experimental observation and analysis of inverse transients for pipeline leak detection, Journal of Water Resources Planning and Management 133 (6) (2007) 519–530.

[14] S. Kim, Impedance method for abnormality detection of a branched pipeline system, Water Resources Management 30 (3) (2016) 1101–1115.

[15] S. H. Kim, A. Zecchin, L. Choi, Diagnosis of a pipeline system for transient flow in low reynolds number with impedance method, Journal of Hydraulic Engineering 140 (12) (2014) 04014063.

[16] J. Gong, A. C. Zecchin, A. R. Simpson, M. F. Lambert, Frequency response diagram for pipeline leak detection: Comparing the odd and even harmonics, Journal of Water Resources Planning and Management 140 (1) (2014) 65–74. doi:doi:10.1061/(ASCE)WR.1943-5452.0000298.

[17] W. Mpesha, S. L. Gassman, M. H. Chaudhry, Leak detection in pipes by frequency response method, Journal of Hydraulic Engineering 127 (2) (2001) 134–147.

[18] M. Ferrante, B. Brunone, Pipe system diagnosis and leak detection by unsteady-state tests. 1. harmonic analysis, Advances in Water Resources 26 (1) (2003) 95–105.

[19] D. Covas, H. Ramos, A. B. De Almeida, Standing wave difference method for leak detection in pipeline systems, Journal of Hydraulic Engineering 131 (12) (2005) 1106–1116.

[20] P. J. Lee, M. F. Lambert, A. R. Simpson, J. P. Vtkovsk, J. Liggett, Experimental verification of the frequency response method for pipeline leak detection, Journal of Hydraulic research 44 (5) (2006) 693–707.

[21] A. M. Sattar, M. H. Chaudhry, Leak detection in pipelines by frequency

response method, Journal of hydraulic research 46 (sup1) (2008) 138–151.

[22] J. Gong, A. R. Simpson, M. F. Lambert, A. C. Zecchin, Determination of the linear frequency response of single pipelines using persistent transient excitation: a numerical investigation, Journal of Hydraulic Research 51 (6) (2013) 728–734.

[23] A. Zecchin, M. Lambert, A. Simpson, L. White, Parameter identification in pipeline networks: transient-based expectation-maximization approach for systems containing unknown boundary conditions, Journal of Hydraulic Engineering 140 (6) (2013) 04014020.

[24] A. C. Zecchin, L. B. White, M. F. Lambert, A. R. Simpson, Parameter identification of fluid line networks by frequency-domain maximum likelihood estimation, Mechanical Systems and Signal Processing 37 (1) (2013) 370–387.

[25] M. Taghvaei, S. B. M. Beck, W. J. Staszewski, Leak detection in pipelines using cepstrum analysis, Measurement Science and Technology 17 (2) (2006) 367.
URL http://stacks.iop.org/0957-0233/17/i=2/a=018

[26] J. D. Shucksmith, J. B. Boxall, W. J. Staszewski, A. Seth, S. Beck, Onsite leak location in a pipe network by cepstrum analysis of pressure transients., Journal: American Water Works Association 104 (8).

[27] I. Stoianov, B. Karney, D. Covas, C. Masksimovic, N. Graham, Wavelet processing of transient signals for pipeline leak location and quantifica-

tion, in: International Conference on Computing and Control for the Water Industry (CCWI 2001).

[28] M. Ferrante, B. Brunone, S. Meniconi, Wavelets for the analysis of transient pressure signals for leak detection, Journal of hydraulic engineering 133 (11) (2007) 1274–1282.

[29] M. Ferrante, B. Brunone, S. Meniconi, Leak detection in branched pipe systems coupling wavelet analysis and a lagrangian model, Journal of Water Supply: Research and Technology-AQUA 58 (2) (2009) 95–106.

[30] J. Urbanek, T. Barszcz, T. Uhl, W. Staszewski, S. Beck, B. Schmidt, Leak detection in gas pipelines using wavelet-based filtering, Structural Health Monitoring 11 (4) (2012) 405–412.

[31] M. Ghazali, S. Beck, J. Shucksmith, J. Boxall, W. Staszewski, Comparative study of instantaneous frequency based methods for leak detection in pipeline networks, Mechanical Systems and Signal Processing 29 (2012) 187–200.

[32] J. Gong, M. F. Lambert, A. C. Zecchin, A. R. Simpson, Experimental verification of pipeline frequency response extraction and leak detection using the inverse repeat signal, Journal of Hydraulic Research (2015) 1–10.

[33] B. Brunone, Transient test-based technique for leak detection in outfall pipes, Journal of water resources planning and management 125 (5) (1999) 302–306.

[34] C. W. Helstrom, Statistical Theory of Signal Detection: International

Series of Monographs in Electronics and Instrumentation, Vol. 9, Elsevier, 2013.

[35] J. Gong, M. F. Lambert, A. C. Zecchin, A. R. Simpson, Experimental verification of pipeline frequency response extraction and leak detection using the inverse repeat signal, Journal of Hydraulic Research 54 (2) (2016) 210–219.

[36] T. Roinila, M. Vilkko, T. Suntio, Frequency-response measurement of switched-mode power supplies in the presence of nonlinear distortions, IEEE Transactions on Power Electronics 25 (8) (2010) 2179–2187.

[37] J. Jegandren, R. Gobbi, H. S. Athab, An investigation on control strategies for fast transient response of smps, in: Innovative Technologies in Intelligent Systems and Industrial Applications, 2008. CITISIA 2008. IEEE Conference on, IEEE, 2008, pp. 110–115.

[38] J. Jegandren, R. Gobbi, H. S. Athab, Voltage injection switching inductor (visi) method for fast transient response in switch mode power supplies, in: Power and Energy Conference, 2008. PECon 2008. IEEE 2nd International, IEEE, 2008, pp. 186–191.

[39] A. Cataldo, G. Cannazza, E. De Benedetto, N. Giaquinto, A new method for detecting leaks in underground water pipelines, IEEE Sensors Journal 12 (6) (2012) 1660–1667.

[40] J. Gong, A. C. Zecchin, M. F. Lambert, A. R. Simpson, Signal separation for transient wave reflections in single pipelines using inverse filters, in: World Environmental and Water Resources Congress 2012: Crossing Boundaries, 2012, pp. 3275–3284.

[41] E. B. Wylie, V. L. Streeter, L. Suo, Fluid transients in systems, Vol. 1, Prentice Hall Englewood Cliffs, NJ, 1993.

[42] J. Osterwalder, C. Wirth, Experimental investigations of discharge behaviour of crack-like fractures in pipes, Journal of Hydraulic Research 23 (3) (1985) 255–272.

[43] J. P. Vitkovsy, M. F. Lambert, A. R. Simpson, J. A. Liggett, Experimental observation and analysis of inverse transients for pipeline leak detection, Journal of Water Resources Planning and Management 133 (6) (2007) 519–530.